INSTITUTE OF PHYSICS PUBLISHING SMART MATERIALS AND STRUCTURES
Smart Mater. Struct. **15** (2006) N137–N146 doi:10.1088/0964-1726/15/6/N01

TECHNICAL NOTE

System for monitoring the evolution of the thermal expansion coefficient and autogenous deformation of hardening materials

M Viviani[1,4], **B Glisic**[2] **and I F C Smith**[3]

[1] GCC Technology and Processes, CH 1400 Yverdon-les-Bains, Switzerland
[2] Smartec SA, CH 6928 Manno, Switzerland
[3] Ecole Polytechnique Fédérale de Lausanne (EPFL), Applied Computing and Mechanics Laboratory, Station 18, CH 1015 Lausanne, Switzerland

E-mail: mviviani@gcc.com

Received 14 January 2006, in final form 14 August 2006
Published 3 October 2006
Online at stacks.iop.org/SMS/15/N137

Abstract
This article presents an experimental system developed to determine the kinetic parameters of hardening materials. Kinetic parameters allow computation of the degree of reaction indices (DRIs). DRIs are used in predictive formulae for strength and are used to decouple the autogenous deformation (AD) and thermal deformation (TD). Although there are several methods to determine values for kinetic reaction parameters, most require extensive testing and large databases. A measurement system has been developed in order to determine kinetic parameters. The measurement system consists of optical fiber sensors embedded in specimens that are cured at varying temperatures and conditions. Sensors are used in pairs inside each specimen, and each pair has two deformation sensors that, aside from their axial stiffness, have the same characteristics. The study of the interaction between sensors and hardening material leads to establishment of a link between the deformations measured and the degree of reaction, by means of the newly developed concept of the equivalency point. The equivalency point is assumed to be an indicator of the degree of reaction and it allows the determination of the apparent activation energy (E_a) which defines the equivalent time. Equivalent time is a degree of reaction index (DRI) and it accounts for the combined effect of time and temperature in concrete. This new methodology has been used to predict the compressive strength and separate the AD and thermal expansion coefficient (TEC) in seven types of concrete. The measurement system allows gathering of data necessary for fast and efficient predictions. Due to its robustness and reduced dimensions it also has potential for *in situ* application.

(Some figures in this article are in colour only in the electronic version)

1. Introduction

A maturity method is used to decouple from the total deformation values for TD, AD and to predict strength (Carino 1991, De Shutter 2005, Turcry *et al* 2002). Maturity methods use degree of reaction indices (DRIs) to evaluate the combined effect of time and temperature in cement hydration. Values for the apparent activation energy are necessary to implement the maturity approach when equivalent time is used as a DRI

[4] Address for correspondence: Av. Des Sciences, Yverdon les Bains, Switzerland.

(Freiesleben Hansen and Pedersen 1977). Determination of E_a usually requires extensive tests. This has resulted in limited use of maturity methods in decoupling techniques and strength prediction.

A new methodology to determine such a value has been proposed (Viviani 2005). The methodology is based on early age measurements of deformation and temperature. A comparative dilatometer has been developed with the scope of monitoring deformations and temperature of hardening materials from the pouring to the hardening. This paper presents details of this dilatometer and shows how it can be used through summaries of studies that are presented in more detail elsewhere (Viviani *et al* 2006a, 2006b). Parameters such as the evolution of strength, autogenous deformation and the thermal expansion coefficient have become reliably measurable at very early stages of hardening using an inexpensive and robust apparatus.

2. Background

At early age, the mechanical properties of cement-based materials are time dependent and involve hydration. The hydration process is a thermally activated reaction that may be described by the Arrhenius equation (see equation (1)). This equation establishes the progression of a chemical reaction in terms of rate of reaction k (Arrhenius 1889):

$$k = A \exp \frac{-E_a}{RT} \tag{1}$$

where A is the frequency factor (s^{-1}), E_a is the activation energy (kJ mol^{-1}), k is the reaction rate, R is the gas constant (kJ mol^{-1} K^{-1}) and T is the absolute temperature (K).

The integral over time of the rate of reaction gives the degree of reaction. The degree of reaction is useful because it quantitatively expresses the effect of time and temperature in concrete. At every degree of hydration some mechanical properties and the chemical shrinkage of a cementitious material are similar, independent of the combination of time and temperature that contributed to that particular degree of hydration for temperatures less than 40 °C. This approximate rule has been widely investigated and successfully applied to the thermal expansion coefficient (TEC), mechanical properties and chemical shrinkage for the first days of hydration. Discussion is still open in the scientific community on the possibility of extending the principle to the complete life of concrete and for all properties including the degree of systematic errors (Bjøntegaard and Sellevold 2001, Kada *et al* 2002, Kjellsen and Detwiler 1993, Loukili *et al* 2000, Regourd and Gautier 1980, Sarkis *et al* 2002, Knudsen and Geiker 1982). For the age considered in this work, the TEC has been found to be the same at the same degree of reaction, as observed for chemical shrinkage. Thus, if two specimens are cured in autogenous conditions (only AD and TD) and hydrate under different temperatures, separation of effects is possible only by converting the time-histories into degree of reaction histories. For technical, practical and economical reasons, testing through degree of reaction is feasible only in the laboratory. Advancement of the hydration is thus computed by degree of reaction indices (DRIs). The most common formulae, such as the equivalent time ((Freiesleben Hansen and Pedersen 1977); see equation (2)) are semi-empirical.

$$Et = \int_{t_0}^{\text{Equ. point}} \left[\exp \frac{-E_a}{R} \left(\frac{1}{T(t)} - \frac{1}{T_{\text{reference}}} \right) \right] \mathrm{d}t \tag{2}$$

where Et is the equivalent age (hours at reference temperature), $T_{\text{reference}}$ is the reference temperature (°C), $T(t)$ is the temperature of the specimen (°C), E_a is the apparent activation energy (kJ mol^{-1}), Equ. point is the equivalency point of the specimen considered (h), R is the gas constant (kJ mol^{-1} K^{-1}), and t_0 the time at the end of pouring (h).

A DRI most easily substitutes for a measured degree of reaction when it has a linear relationship with the degree of reaction. Schindler, in a recent article, shows that the second formulation of Freisleben-Hansen equivalent time is particularly suitable to be a DRI (Freiesleben Hansen and Pedersen 1985, Schindler 2004a) since it shows linearity at any age with the measured degree of reaction (Schindler 2004a). While the equivalent time might be less representative at very early age than other indices, correlation is improved with the use of appropriate techniques for determining the initial time t_0 (Schindler 2004a, Mounanga *et al* 2006, Weiss 2002, Byfors 1980) and the apparent activation energy (see Schindler 2004a). Maturity is historically very important (Saul 1951) and has been shown to be conceptually coincident with the equivalent time (De Shutter 2005). A new technique is developed to determine the driving parameters of DRIs and in particular the apparent activation energy E_a, which is a fundamental parameter in the Freisleben equivalent time calculation. This technique is based on measurement of early age deformations and temperatures.

The evolution of the compressive strength in term of DRIs has been studied since the 1950s, when Saul, Mcinthosh and Nurse developed the concept of maturity for accelerated curing of concrete. The most useful formula has been developed mathematically and proposed independently by Knudsen and Carino on the basis of Bergstrom's work:

$$S(k_r, t) = S_u \frac{k_r(t - t_0)}{1 + k_r(t - t_0)} \tag{3}$$

k_r is the rate of reaction at the reference temperature T_r, S is the compressive strength at age t (MPa), S_u is the ultimate compressive strength (MPa), t_0 is the age at start of strength development (h) and t is the time (h).

A methodology has been developed to determine the initial time t_0 and the rate constant k_r. This methodology is based on the measurement at two different equivalent times of the compressive strength. Deformations are measured by a pair of embedded optical fiber sensors. The two sensors have the same characteristics except for axial stiffness. Therefore they are called soft and stiff sensors. Previous work proposed the determination of a hardening curve through plotting the difference between the soft and stiff sensors' deformation-time history (Glisic 2000, Glisic and Simon 2000, Viviani *et al* 2005). When using this method difficulties were encountered in terms of defining the hardening time reliably for some types of concrete.

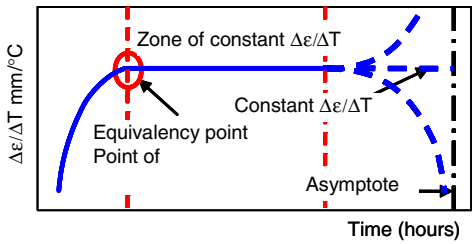

Figure 1. Predicted shape of the $\Delta\varepsilon/\Delta T$ curve (Viviani *et al* 2006a).

3. Methodology

The new methodology is based on the equivalency points. Using the same apparatus that was used to find hardening times, equivalency points are determined using temperature and deformation measurements inside a specimen of concrete. The hardening curve is calculated and divided by the temperature variation–time history. The resulting graphs have a curve that begins with a steep increase and then levels off to a constant value (see figure 1). Later, a delta temperature or deformation approaching zero produces a vertical asymptote. The equivalency point is defined by the point at which a line drawn on the plateau of the $\Delta\varepsilon/\Delta T$ curve departs from the curve on the left side.

The equivalency point is assumed to be related to the degree of reaction. This assumption is made on the basis of the mechanism of deformation transferring between hardening material and sensors (Viviani *et al* 2006a). This means that at the equivalency point the degree of reaction is the same for all specimens of the same material hydrating in autogenous conditions, and is independent of the combination of time and temperature that leads to a given degree of reaction. Determination of E_a requires detection of the equivalency point in two specimens made of the same hardening material and reacting at different speeds (see figure 2). Once E_a is known, very early age deformation data can be decoupled into parts that are related to different physical phenomena (AD, TEC). Furthermore, using equation (3), prediction of compressive strength evolution after three days of measurements is possible.

3.1. Predictions of compressive strength

The apparent activation energy is necessary but not sufficient for determining the rate constant k_r (see equation (1)). The value of k_r is needed to predict mechanical properties (see equation (3)). It can be determined if two compressive tests using standard specimens of the same composition are performed at different equivalent ages Et. This allows determination of k_r through the application of equation (3) (see figure 3). Compressive tests have been carried out after 48 and 72 h (with exception of test 1 where the tests were made at 24 and 72 h). The 24 h test has not been found to be representative for slowly hydrating concrete. Zero equivalent age in equation (3) is not always the pouring time. A newly poured concrete temperature is influenced mainly by the temperature of the surrounding ambient during the first hours of life. Thus the zero equivalent age is the time where cooling (if it occurs) slows to a variable rate. In cases where no cooling occurs, the zero time is taken to be the batching time.

3.2. Separation of effects

Total deformation of specimens cured in 'autogenous conditions' is the sum of thermal and autogenous deformation (TD and AD):

$$\varepsilon(Et) = \varepsilon_{ad}(Et) + \mathrm{TEC}(Et) * \Delta T(Et) \qquad (4)$$

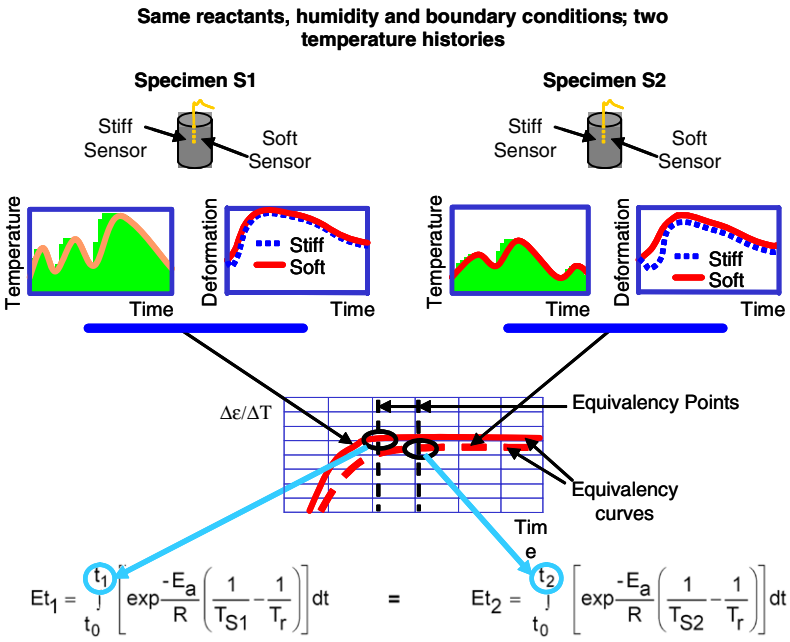

Figure 2. Determination of the activation energy E_a (Viviani *et al* 2006a).

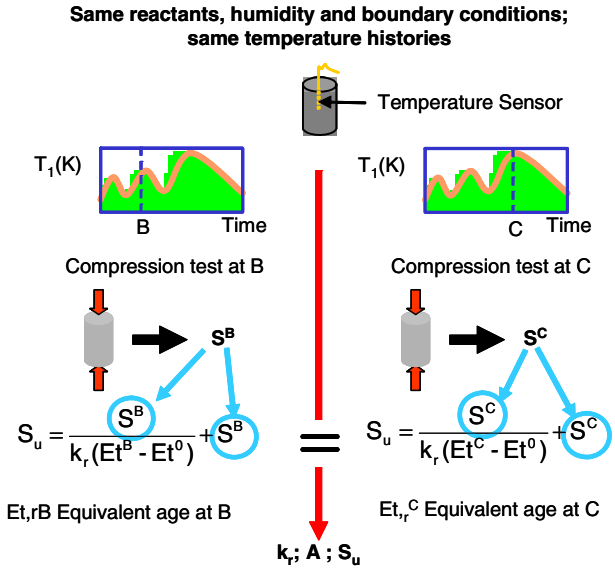

Figure 3. The determination of K_r and S_u (Viviani *et al* 2006a).

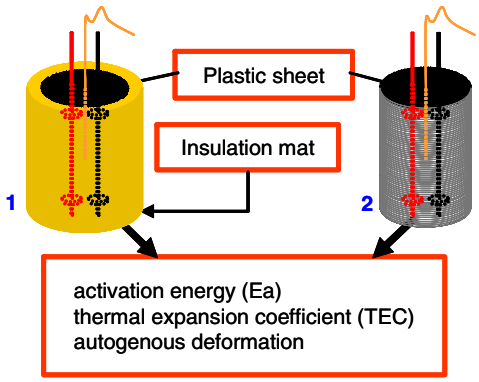

Figure 4. A schema of the comparative dilatometer (Viviani *et al* 2006b).

where TEC is the thermal expansion coefficient (μm m^{-1} °C^{-1}), ΔT is the rise in temperature from the initial time (°C), ε_{ad} is the autogenous deformation (μm m^{-1}), ε is the total deformation measured (μm m^{-1}) and Et is the equivalent time of the concrete (h).

If the temperature of hydration is kept artificially constant, the AD and total deformation are equivalent since there is no thermal deformation. Many systems have been proposed to measure the AD directly and its evolution has been measured for a range of cement based materials. At varying temperature, the time scale can be substituted with a DRI scale, using the equivalent time (see equation (2)). If the AD and the TEC are found to be functions of a DRI, the TEC can be determined by comparing the total deformation of two cylinders hydrating at different temperatures (see figure 4, equation (4)).

4. The comparative dilatometer

To determine the rate of reaction k_r and apparent activation energy, measurements of deformations and temperature of hardening materials are necessary. Furthermore deformations measured in specimens provide the total deformations used

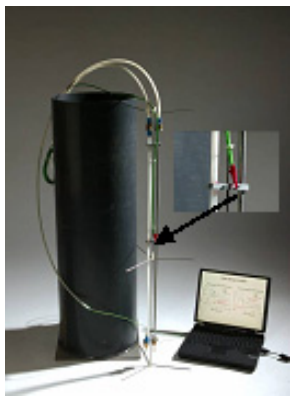

Figure 5. The standard and stiff sensors (Viviani *et al* 2005).

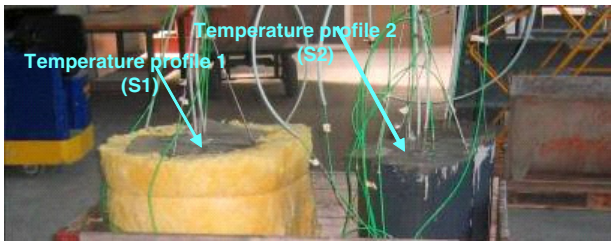

Figure 6. Specimens under test (Viviani *et al* 2006a).

in separations. It is thus important to measure deformations and temperatures as exactly as possible as well as to estimate measurement errors.

Hardening materials have a viscous consistency when poured. Embeddable sensors measure deformations efficiently in such materials. Sensors need to be directly coupled with the material, have a low axial stiffness, and be insensitive to magnetic fields and humidity. Insensitivity to magnetic fields is a requirement in field applications where there are many sources of magnetic fields that perturb the sensors. Temperature compensation must be easy to perform or automatic. Work has already been done on monitoring hardening material deformations using embeddable fibre-optic sensors (Inaudi 1997). Furthermore, constraints given by the testing apparatus to concrete must be minimal. Thus moulds and curing procedures are fundamental to ensure that the material condition of specimens are the closest possible to a free hydration of concrete. Moulds are standard pipes for water conduction. They are robust, cheap and made of a material that has a high thermal expansion coefficient (Viviani 2005).

The comparative dilatometer has been built using large cylindrical PVC moulds (see figure 5). A system to hold and position the sensors (deformation and temperature) inside the mould has been developed. One of the cylinders has been wrapped with an insulation mat in order to force different temperatures of hydration in the two specimens. Tests were carried out to estimate the influence of the mould on the hardening material and the effect of their characteristics on the measurements. Even though the moulds used are larger than standard moulds, they can be placed on a standard pallet, and this helps ensure they are protected from excessive air flow (see figure 6). In summary, the moulds, even if unusual in

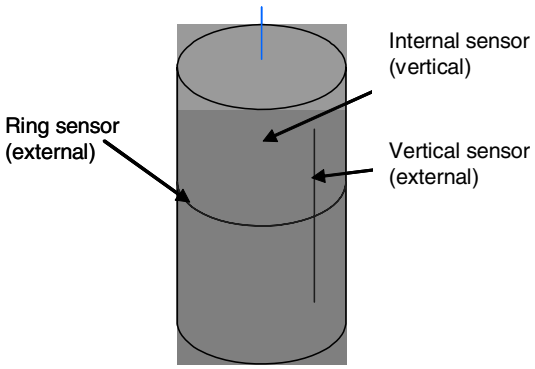

Figure 7. Monitoring of the mould M2.

concrete technology, are appropriate for use for deformation measurement of concrete at early age. The potential for use in the field is also very good.

4.1. Effect of moulds on the hardening material

Testing was carried out to determine whether or not moulds constrain concrete. Figure 7 shows sensor positions for a test performed on moulds where the internal and external deformations were measured on two specimens, one wrapped with an insulation mat and one uncovered. Figure 8 refers to the specimen wrapped with the insulation mat. Both specimens were protected against drying with plastic sheets. Temperature was monitored. At early age and for the whole hydration phase, the mould expands more than the concrete. The deformation of concrete is consistent with the phase of hydration and showed no anomalous settlement. Within the same test session, the deformation of mould was measured for two specimens hardening with a different temperature profiles. In both specimens at early age, there is a discontinuity in the deformation of the mould (see figure 8). This is the moment when the mould detaches from the fresh concrete and this might approximate the moment when the self-supporting skeleton develops (final setting time). The detachment of the mould from the concrete at early age allows free deformation of the concrete specimen. A mould with thermal expansion coefficient that is lower than concrete in the hardening phase would have constrained the specimen and perturbed the strain field.

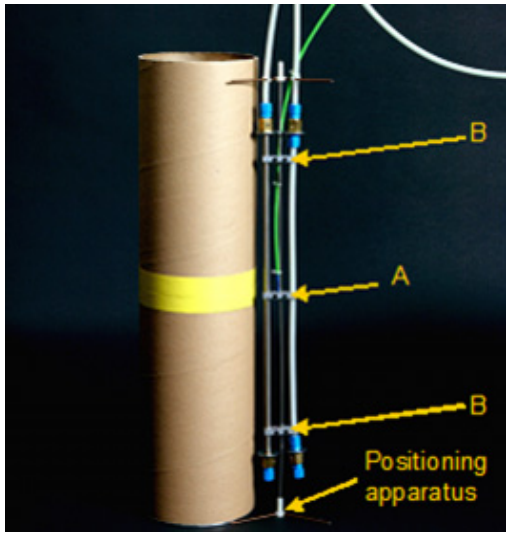

Figure 9. Positioning parts for soft and stiff sensors in a paper box mould.

4.2. Positioning-holding apparatus

Deformation measurement of fresh concrete requires the use of sensors that are directly coupled with the material with a minimum effect from the holding and positioning system. The positioning apparatus designed for cylinder specimens (see figure 9) supports the sensors in the middle by part A, while parts B have the function of keeping the sensors straight during pouring and vibration of the concrete. Parts B are not attached rigidly to the sensors. The positioning apparatus studied is made from thin rods of stainless steel of 2.5 mm diameter. Such rods have little effect on the concrete behaviour because they have a small cross-sectional area (0.74 cm^2), they are smooth and they are treated with grease before pouring to reduce concrete adhesion.

4.3. Temperature measurement

Temperature was measured with K-type thermocouples. The data acquisition system allowed temperature and deformation to be measured at the same time. All calculations have been made assuming a constant temperature over the section. This assumption has been verified during a test where the external

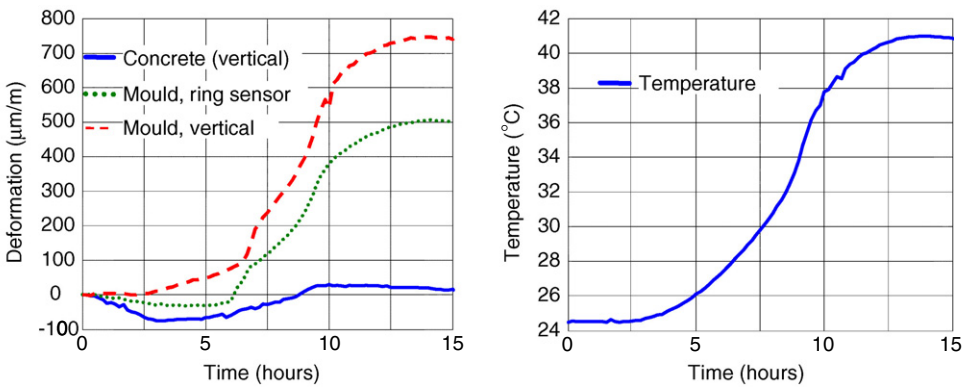

Figure 8. Characteristics of mould M2, temperature profile 2 (first 15 h).

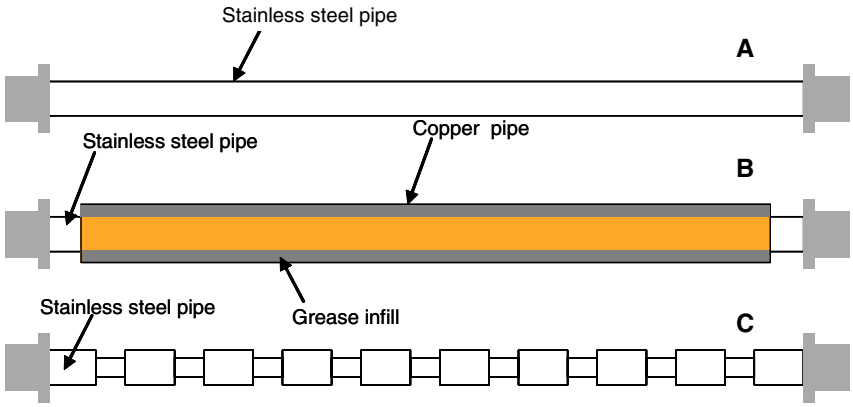

Figure 10. Three types of stiff sensor.

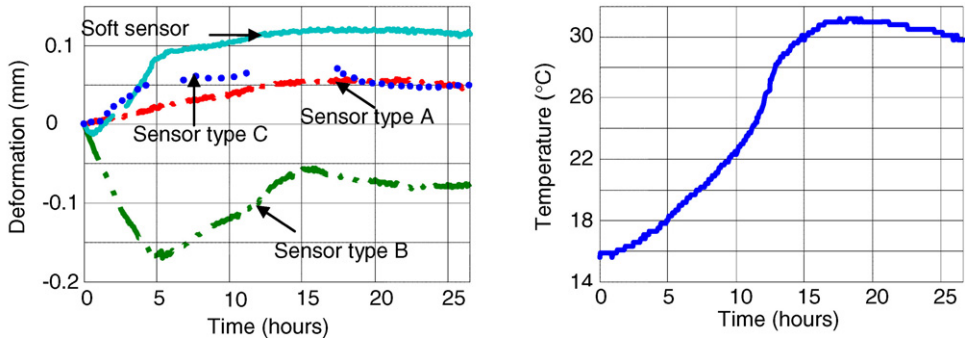

Figure 11. Deformations of the four sensors in figure 10 and temperature of the specimens at the sensor location.

temperature suddenly varied by 10 °C. The variation between the side and the centre of the specimen was of maximum 1 °C. Temperature distortion is proportional to the current thermal expansion coefficient of concrete (this varies with the hydration stage) and the temperature variation.

4.4. Curing

Two moulds are used in each experiment. The separation of effects via the degree of reaction history requires suppressing one condition at a time. Thus, the effect of the suppressed condition on the total deformation is measured. The first specimen is protected during curing against the loss of moisture by a plastic sheet that covers the air-exposed surfaces, and is wrapped with a thick layer of glass wool (insulating mat) in order to increase the hydration temperature naturally (see specimen S1, figure 6). The second specimen is protected against moisture loss (as for the first specimen) but does not have an insulation mat. The third specimen is left without any moisture-loss protection or insulating mat. This allows two temperature profiles and two moisture-curing profiles to be measured and relative influences identified.

4.5. Sensor anchor piece influence

The detection of equivalency points is based on the sensor-hardening material exchange of forces occurring at the interface between the two materials. The influences of the sensors' anchor pieces have not been taken into account. In order to study the influence of the anchor pieces, a comparative test was performed. Four sensors having varying stiffness and surface roughness have been prepared. The first is a soft sensor, the second a stiff sensor with smooth surface (type A in figure 10). The third is a stiff sensor inserted in a larger copper pipe, with the gap filled of grease (type B in figure 10). The fourth is a stiff sensor with the section reduced at regular distances, such that a roughness is created (type C in figure 10). All the sensors have 500 mm of active length and have been installed in a parallelepiped mould.

The results show that the sensor type B is dominated by the thermal expansion coefficient of steel and the 'piston' effect made by the anchor pieces. The temperature of the newly mixed concrete was much lower of the sensor B and ambient temperature (concrete 16 °C, sensor and ambient 24 °C). This made the sensor adapt to the concrete temperature with a large and unrestrained shrinkage (anchor pieces immerse in fresh concrete, no friction between the protective pipe and the fresh concrete). Afterwards, the rising temperature and the absence of friction with the surrounding concrete led to an elongation of the sensor. The swelling was reduced in magnitude by the anchor pieces that, in direct contact with the concrete matrix, are not free to move.

It is also interesting to highlight the behaviour of the sensor type C, which is softer than type A. The mechanism of force transfer is a mix between interfacial and anchor (see figure 11). The deformation measured by the sensor type C is higher than the measured by the sensor type B due to the higher contact surface exposed to the hardening concrete. More specifically, the difference in behaviour between sensor

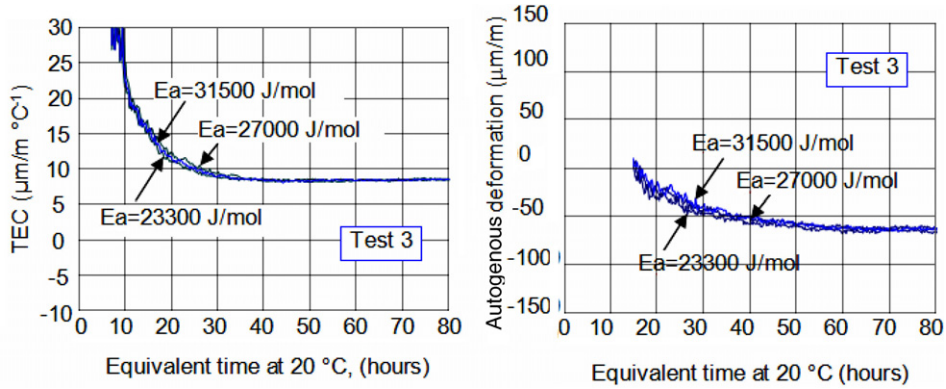

Figure 12. Examples of thermal expansion coefficient evolution (TEC) (Viviani *et al* 2006b).

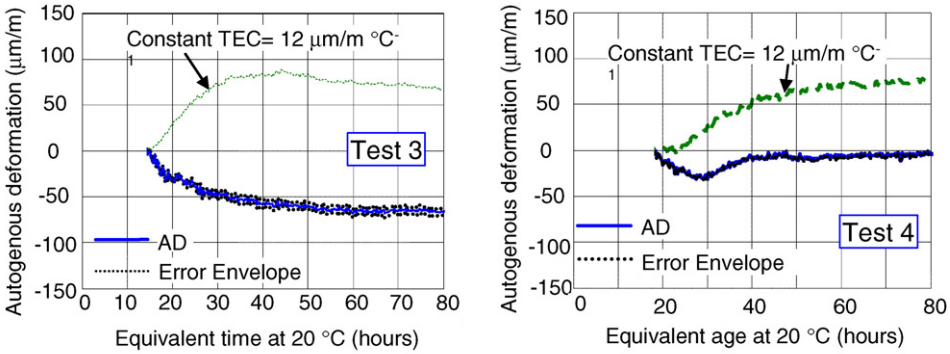

Figure 13. Examples of autogenous deformation evolution: positive values are contractions (Viviani *et al* 2006b).

types B and C indicates that the adherence effect along the length of the sensor is important.

Finally, the time histories of the sensors shown in figure 10 demonstrate that the characteristics of the sensors' external surface may have an important influence on the deformation measured. Therefore, the sensor surface characteristics have an influence on the time when the equivalency point occurs and this could therefore be a monitoring parameter for adjustment according to measurement objectives.

5. Estimation of errors

Measurement errors (two standard deviations from mean) have been estimated for deformations and temperature using experimental values. Measurement noise when reading deformation and temperature as well as time-dependent drift are especially important when deformation and temperature readings are added, subtracted, multiplied or divided, since errors can amplify to become high percentages of results that are reported. Propagation of errors has been estimated in order to construct the error envelope for TEC (and for autogenous deformation). The equivalent error, Δs, for addition and subtraction of quantities A and B is calculated as follows:

$$\Delta s = \sqrt{\Delta A^2 + \Delta B^2} \tag{5}$$

where Δs is the equivalent error related to results of addition or subtraction of quantities A and B; ΔA is the error related to measuring quantity A; ΔB is the error related to measuring quantity B.

For multiplication and division of quantities A and B the error is calculated as follows:

$$\Delta r/r = \sqrt{\left(\frac{\Delta A}{A}\right)^2 + \left(\frac{\Delta B}{B}\right)^2}. \tag{6}$$

Δr is the error related to results of multiplication or division of the quantities A and B.

The error envelope, calculated on the basis of two standard deviations from mean measurement, shows that the errors have little effect on values of the TEC as well as on values of AD (see figures 12 and 13).

E_a is determined using the equivalency point on two specimens. Because Et at the equivalency point is assumed to be the same for both specimens, E_a can be determined. Errors in the determination of the equivalency point might result in poor predictions of apparent activation energy. Drift and noise related to measurements introduce an error in terms of time on the equivalency point. The worst case scenario for the calculation of the apparent activation energy corresponds to the following bounds on values for the equivalency points:

$$Ep = Ep \pm 6 \text{ min}.$$

This leads to two bounds on the apparent activation energy. The worst case scenario on values for the apparent activation energy is used to determine the effect on values calculated for TEC, AD and strength.

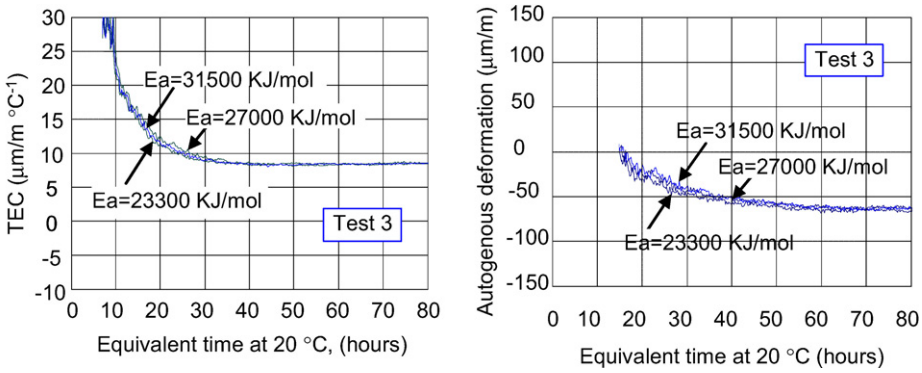

Figure 14. Effect of apparent activation energy variation (Viviani *et al* 2006b).

Table 1. Mix-design test 1-07 (from Viviani *et al* 2006a).

	Test 1	Test 2	Test 3	Test 4	Test 5	Test 6	Test 7
Water/cement ratio	0.45	0.45	0.48	0.48	0.48	0.18	0.43
Cement	325 kg m^{-3}	350 kg m^{-3}	360 kg m^{-3}	360 kg m^{-3}	360 kg m^{-3}	1051.1 kg m^{-3}	420 kg m^{-3}
Cement type	CEM II/A-LL 42.5 R	CEM I 42.5 R	CEM I 42.5 N HS	CEM III/A 32.5 N	CEM II/ A-LL 32.5 R	CEM I 52.5 N HTS	—
Superplasticizer	0.9%	0.8%	0.8%	0.8%	0.8%	35.1 kg m^{-3}	—
Air entrainer	0.1%	—	—	—	—	—	—
Aggregate	0–32 Hüttwangen	0–32 Sergey	0–32 Sergey	0–32 Sergey	0–32 Sergey 0–32 Sergey	0–4 sand of Fontainebleau	0–32 Sergey
Silica fume	—	—	—	—	—	273.3 kg m^{-3}	—
Steel fibre	—	—	—	—	—	Yes[a]	—
Maximum temperature difference	5 °C	15 °C	20.2 °C	14.5 °C	21.6 °C	14.5 °C	30 °C

[a] For further details of the mix-design of this test, see Habel (2004).

6. Test results

Tests have been carried out on seven different types of concrete (Viviani 2005, Viviani *et al* 2005). Activation energy and separation of TD and AD have been performed for five types of concrete. Predictions of compressive strength have been made for seven types of concrete. Mix designs are presented in table 1. Examples of results are described briefly below.

6.1. Separation of AD and TD

A literature review has identified two typical shapes for TEC evolution. The first shape is described by Byfors (1980), Laplante and Boulay (1994) to be a rapid decrease of the TEC in the first 10 equivalent time hours, then a leveling off to the TEC values typical of mature concrete (5–12 μm m^{-1} $°C^{-1}$) at around 10 to 15 equivalent time hours. Figure 12 shows examples of TEC evolution.

Examples of autogenous deformation evolution are given in figure 13. Tests have a swelling phase that ends at 80 h for test 3 and levels off at 40 h for test 4. In the first hours of the cement-based material life, the AD can be an expansion. The same calculation made using the evolution of the TEC shown in figure 13 are repeated using a constant TEC (of 12 μm m^{-1} $°C^{-1}$), with surprising results. Using constant values for the TEC in the calculation, AD expansion is not observed, whereas on using the experimentally determined TEC, expansion occurs in all tests. The effect of the apparent activation energy variation on TEC and AD evolutions is shown in figure 14. Results are not influenced by substantial changes in values of apparent activation energy.

Table 2. Final setting times (initial time t_0) for tests 1–5 (Viviani *et al* 2006b).

Test	α_{cr} (% of degree of reaction)	Setting times (h)
1	18	15.1
2	18	9.1
3	19.2	14.5
4	12.5	18.9
5	4.7	1.35

Final setting time has been evaluated to be when the degree of reaction is $\alpha = 0.26$ (w/c) for slag cements and silica fume incorporation in the mix while for other cement types the critical degree of reaction is $\alpha = 0.40$ (w/c), as presented in Schindler (2004b), Byfors (1980) and Pinto and Hover (1999). Values for final setting time are presented in table 2.

The comparative dilatometer presented in this paper is thus a practical method to determine the thermal expansion coefficient. The values of TEC obtained are consistent with

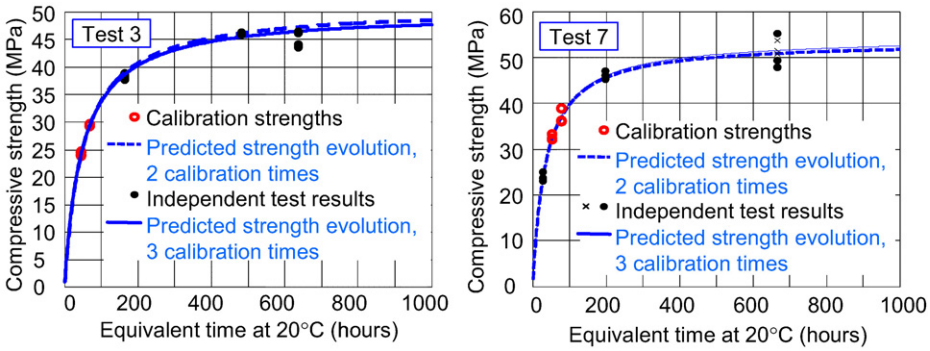

Figure 15. Examples of compressive strength versus equivalent age. Calibration strengths of young concrete are used to predict strength evolution and this prediction is verified by independent test results using cylinders containing more mature concrete (Viviani *et al* 2006a).

values found in the literature. TEC values are used to separate values for autogenous deformation from values of total deformation. The AD obtained is very different from the ones commonly expected and indicate expansions in some cases. Expansion can last for 80 h (Et at 20 °C). Although the propagation of worst case scenarios errors (on measurements and apparent activation energy values) might lead to errors in values for AD and TEC, they are not enough to change the form of the curves.

6.2. *Prediction of compressive strength*

The equivalency point, apparent activation energy and rate of reaction were evaluated and applied to seven different types of concrete (see table 1) using the procedure presented above. Five were commonly used concrete types in civil engineering. They were made with different types of aggregate. Air entrainers, superplasticizers and different types of cements were used (see table 1). The results shown in figures 15 are examples of what can be obtained within the first 72 h. All predictions obtained were realistic and acceptable without any correction according to the criteria given in the manual TxDOT 404-A (Texas Department of Transportation 2004).

7. Conclusions

A new comparative dilatometer has been developed. The new moulds and positioning system designed show the capability of monitoring early and very early age deformations of hardening material. Sensors have been designed to allow the detection of the equivalency points and this capacity has lead to a new methodology that determines the apparent activation energy. The use of the new apparatus permits measurement of the data necessary to predict strength and separate effects. Finally, the equipment is reusable and robust and, therefore, inexpensive and *in situ* applications of the methodology have become feasible.

Acknowledgments

This project was supported in its early stages through a project funded by the Swiss Commission for Technology and Innovation (CTI) and Cemsuisse (Swiss Cement Fabricators Association). The authors are grateful to Professor Karen Scrivener, EPFL, for valuable advice and for providing testing support. We also express special thanks to Patrice Gallay who has helped design and build the testing apparatus.

References

Arrhenius S 1889 On the reaction velocity of the inversion of cane sugar by acids *Z. Phys. Chem.* **4** 226–32 (as translated and published in Back M H and Laidler K J 1967 Selected Readings in Chemical Kinetics (Oxford: Pergamon))

Bjøntegaard Ø and Sellevold E 2001 Interaction between thermal dilation and autogenous deformation in high performance concrete *Mater. Struct.* **34** 266–72

Byfors J 1980 *Plain Concrete at Early Ages* (Stockholm: CBI Research Swedish Council For Building Research)

Carino N J 1991 The maturity method *CRC Handbook of Non-Destructive Methods* (Boca Raton, FL: CRC Press) pp 101–46

De Shutter G 2005 Applicability of degree of hydration concept and maturity method for thermo-visco-elastic behaviour of early age concrete *Cement Concr. Compos.* **27** 437–43

Freiesleben Hansen P and Pedersen J 1977 Maturity computer for controlled curing and hardening of concrete *Nordisk Betong* **1** 19–34

Freiesleben Hansen P and Pedersen E J 1985 *Curing of Concrete Structures* (Switzerland: CEB)

Glisic B 2000 Fibre optic sensors and behaviour in concrete at early age *PhD Thesis No 2186* EPFL, Lausanne, Switzerland

Glisic B and Simon N 2000 Monitoring of concrete at very early age using stiff SOFO® sensor *Cement Concr. Compos.* **22** 115–9

Habel K 2004 Structural behavior of elements combining ultra-high performance fibre reinforced concrete (UHPFRC) and reinforced concrete *PhD Thesis* EPFL, Lausanne Switzerland

Kada H, Lachemi M, Petrov N, Bonneau O and Aïtcin P C 2002 Determination of the coefficient of thermal expansion of high performance concrete from initial setting *Mater. Struct.* **35** 35–41

Kjellsen K O and Detwiler R 1993 Later-age strength prediction by a modified maturity model *ACI Mater. J.* **90** 220–7

Knudsen T and Geiker M 1982 Chemical shrinkage as an indicator of the stage of hardening *Int. RILEM Conf. on Concrete of Early Ages* vol I (Paris: Ecole National des Pouts et Chaussées) pp 163–7

Inaudi D 1997 Fiber optic sensor network for the monitoring of civil engineering structures *PhD Thesis No. 1612* EPFL, Lausanne, Switzerland

Laplante P and Boulay C 1994 Evolution du coefficient de dilatation thermique du béton en fonction de sa maturité aux tout premiers ages *Mater. Struct.* **27** 596–605

Loukili A, Chopin D, Khelidj A and Le Touzo J Y 2000 A new approach to determine autogenous shrinkage of mortar at an early age considering temperature history *Cement Concr. Res.* **30** 915–22

Mounanga P, Baroghel-Bouny V, Loukili A and Khelidja A 2006 Autogenous deformations of cement pastes: Part I. Temperature effects at early age and micro–macro correlations *Cement Concr. Res.* **6** 110–22

Pinto R C A and Hover K C 1999 Application of maturity approach to setting times *ACI Mater. J.* **96** 686–91

Regourd M and Gautier E 1980 Comportement des ciments soumis au durcissement accéléré *Ann. l'Institut Bât. Travaux Publics* **387** 83–96

Sarkis M, Granju J L, Arnaud M and Escadeillas G 2002 *Coefficient de dilatation thermique d'un mortier frais Mater. Struct.* **35** 415–20

Saul A 1951 Principles underlying the steam curing of concrete at atmospheric pressure *Mag. Concr. Res.* **2** 127–40

Schindler A 2004a Effect of temperature on the hydration of cementitious materials *ACI Mater. J.* **101** 72–81

Schindler A 2004b Prediction of concrete setting *RILEM Int. Symp. on Advances in Concrete Through Science and Engineering (Evanston, IL, 2004)*

Texas Department of Transportation 2004 *Tex-426-A, estimating concrete strength by the maturity Method. Manual of concrete testing procedures 400-A* available at the address: http://manuals.dot.state.tx.us/dynaweb/colmates/mtp/@Generic__BookTextView/97151 last access 12-12-2005

Turcry P, Loukili A, Barcelo L and Casabonne J M 2002 Can the maturity concept be used to separate the autogenous shrinkage and thermal deformation of a cement paste at early age? *Cement Concr. Res.* **32** 1443–50

Viviani M 2005 Monitoring and modeling of construction materials during hardening *PhD Thesis No. 3168* EPFL, Lausanne Switzerland

Viviani M, Glisic B and Smith I F C 2005 Three-day prediction of concrete compressive strength evolution *ACI Mater. J.* **102** 231–36

Viviani M, Glisic B, Scrivener K L and Smith I F C 2006a Equivalency points: predicting concrete compressive strength evolution in three days *Cement Concr. Res.* submitted

Viviani M, Glisic B and Smith I F C 2006b Separation of thermal and autogenous deformation at varying temperatures using optical fiber sensors *Cement Concr. Compos.* submitted

Weiss W J 2002 Experimental determination of the 'Time-Zero' *Early Age Cracking in Cementitious Systems RILEM State of the Art Report TC-EAS* ed A Bentur, pp 193–5